crystals

MDPI

Article

Rhodamine B Removal of TiO_2@SiO_2 Core-Shell Nanocomposites Coated to Buildings

Dan Wang [1], Zhi Geng [1], Pengkun Hou [1], Ping Yang [2], Xin Cheng [1,*] and Shifeng Huang [1,*]

[1] Shandong Provincial Key Laboratory of Preparation and Measurement of Building Materials, University of Jinan, Jinan 250022, Shandong, China; mse_wangd@ujn.edu.cn (D.W.); gyhhh_8010@163.com (Z.G.); mse_houpk@ujn.edu.cn (P.H.)

[2] College of Materials Science and Engineering, University of Jinan, Jinan 250022, Shandong, China; mse_yangp@ujn.edu.cn

* Correspondence: mse_chengx@ujn.edu.cn (X.C.); mse_huangsf@ujn.edu.cn (S.H.)

Received: 13 January 2020; Accepted: 28 January 2020; Published: 31 January 2020

Abstract: Surface application of photocatalyst in cement-based materials could endow it with photocatalytic properties, however, the weak adhesion between photocatalyst coatings and the substrates may result in poor durability in outdoor environments. In this study, TiO_2@SiO_2 core-shell nanocomposites with different coating thicknesses were synthesized by varying the experiment parameters. The results indicate that SiO_2 coatings accelerated the rhodamine B removal to a certain extent, owing to its high surface area; however, more SiO_2 coatings decreased its photocatalytic efficiencies. The cement matrix treated with TiO_2@SiO_2 core-shell nanocomposites showed good photocatalytic efficiency and durability after harsh weathering processing. A reaction mechanism was revealed by the reaction of TiO_2@SiO_2 nanocomposites with $Ca(OH)_2$.

Keywords: photocatalysis; core-shell structure; TiO_2/SiO_2 composite nanoparticles; cement-based materials

1. Introduction

The application of TiO_2 nanoparticles in cementitious materials has gained considerable interest and research, which could endow it with photocatalytic properties, such as self-cleaning [1], air-purifying [2], and antibacterial properties [3]. P25, a commercial TiO_2 nanoparticle, was widely employed in building materials, owing to its small size, excellent photocatalytic efficiency, being toxic-free, accessible, and affordable merits [4,5]. Poon [6] reported that P25 was used to modify the concrete surface of self-compacting mortars, and it was found to be effective in rhodamine B (RhB) degradation under UV and strong halogen light irradiation. Sánchez [7] mixed P25 into cement mortar using different dosages, and the mortars show outstanding degradation of NO_x gases.

Traditionally, photocatalytic materials are introduced into cement-based materials via a direct mixing method. The obtained TiO_2-containing cement-based materials show accelerated cement hydration [8], lower porosity, improved mechanical properties [9], self-cleaning [10], air-purifying [11], and antibacterial properties [3]. However, the incorporation method faces a serious restriction in having limited photocatalytic efficiency and some conditions. Boule [12] studied TiO_2-containing cement-based materials prepared using different techniques, and the results show that the TiO_2-cement mixture has significantly less efficiency than TiO_2 slurries for the degradation of 3-nitrobenzenesulfonic acid and 4-nitrotoluenesulfonic acid. This is attributed to the reduction in the active surface. Meanwhile, the incorporation method is not applied in existing buildings and natural stone structures.

Enriching the surface of cement-based materials with a photocatalyst seems to be a viable option. However, the weak adhesion of the photocatalytic material to its substrate remains a big concern [13].

When the photocatalyst is exposed to harsh weather, the issue of adhesion gains more importance than it deserves. A binder of cement-based materials with a photocatalyst could be considered in order to improve durability. SiO_2 as an inorganic material is a valuable resource to prevent the release of the TiO_2 photocatalyst from the surface of cement-based materials to the environment, owing to its pozzolanic activity. Meanwhile, the adding of SiO_2 as a heterogeneous catalysis, such as TiO_2@SiO_2 and SiO_2@TiO_2, may improve the photocatalytic efficiency in comparison to pure TiO_2 [14–16]. Stephan [17] obtained silica-titania core-shell composites, and the results show that some core-shell particles have higher photocatalytic efficiency than pure nano-titania photocatalysts. Mendoza [18] studied a cement matrix treated with TiO_2 and TiO_2–SiO_2, which showed high RhB photodegradation conversions (above 80%). Sikora [19] reported that silica/titania ($mSiO_2/TiO_2$) core-shell nanocomposites improved the compressive strength, reduced the water absorption of cement mortars, and exhibited relatively good bactericidal properties.

In this study, TiO_2@SiO_2 core-shell composites with different coating thicknesses were designed and synthetized. SiO_2 coating accelerated RhB removal to a certain extent, and improved photocatalytic durability by test efficiencies before and after curing and an accelerated weathering process. A reaction mechanism was revealed by the reaction of TiO_2@SiO_2 nanocomposites with $Ca(OH)_2$.

2. Experimental Details

2.1. Materials

White Portland cement (WC, P.W 42.5R) was provided by the Aalborg cement company (Jinan, China), and the major chemical compositions of WC are shown in Table 1. Tetraethyl orthosilicate (TEOS), aqueous ammonia (25%), RhB, calcium hydroxide ($Ca(OH)_2$), and absolute ethanol of chemical grade were purchased from China National Pharmaceutical Group Corporation (Beijing, China).

Table 1. Major chemical compositions of withe Portland cement.

Constituent	CaO	SiO_2	SO_3	Al_2O_3	MgO	Fe_2O_3	TiO_2	K_2O	Na_2O
Mass (wt. %)	65.44	20.09	4.07	2.55	1.77	0.25	0.33	0.24	0.71

2.2. Synthesis of TiO_2@SiO_2 Nanocomposites

Commercial TiO_2 nanoparticles (P25) were used as the core structure, and the SiO_2 shell was obtained by the typial Stöber method. P25 (0.1 g) was dispersed into the solution of water (100 mL) and ethanol (80 mL) with an ultrasonic dispersion instrument for 30 min. Aqueous ammonia (1 mL) and TEOS (1 mL) were dropped above the mixture, respectively, under stirring for 8 h at 25 °C. TiO_2@SiO_2 nanocomposites were collected from the solution by a centrifugation method. All the experimental processes were the same, except for the experimental temperature, and nanocomposites obtained at 0 °C were prepared. Experimental parameters, such as temperature and the amount of P25, were adjusted to prepare different nanocomposites, and the detailed experimental data were listed in Table 2.

Table 2. Experimental parameters of TiO_2@SiO_2 nanocomposites.

Parameters TiO2@SiO2	P25 (g)	TEOS (mL)	Water (g)	Ethanol (mL)	NH3·H2O (mL)	Temperature (°C)	Main Thickness of the Shells (nm)	Surface Areas ($m^2 \cdot g^{-1}$)
Sample 1	0.05	0.3	100	80	1	25	3.92	96.63
Sample 2	0.10	0.3	100	80	1	25	2.25	46.63
Sample 3	0.15	0.3	100	80	1	25	1.95	46.49
Sample 4	0.05	0.3	100	80	1	0	6.13	110.42
Sample 5	0.10	0.3	100	80	1	0	4.17	99.75
Sample 6	0.15	0.3	100	80	1	0	3.70	91.42

2.3. Cement Paste Preparation, Curing and Surface Treatment

WC pastes (4 cm × 4 cm × 16 cm) were prepared, and the weight ratio of water to cement was 0.35. The paste specimens were put into a curing chamber at 95% relative humidity and 20 ± 2 °C for 28 days. After that, theses specimens were cut into slices with a size of 4 cm × 4 cm × 2 cm and then dried at 50 °C for 24 h. Pure P25 (0.025 g) and TiO_2@SiO_2 nanocomposites were dispersed into water (2 mL), respectively, and the dosages of nanocomposites were calculated to keep the same concentration of TiO_2, compared to pure P25 suspension. The obtained P25 and TiO_2@SiO_2 suspensions were sprayed on one surface (4 cm × 4 cm) of silices.

2.4. Characterization

Transmission electron microscope (TEM, FEI G2F20, Hillsboro, OR, USA) was employed to observe the morphologies of TiO_2@SiO_2 nanocomposites. Scanning electron microscope (SEM, ZEISS EVO LS15, Germany) was applied to obtain morphological images of the treated cement. N_2 adsorption-desorption isotherms were performed at −196 °C using a multi-function adsorption instrument (BET, Beijing Builder Company MFA-140, Beijing, China). The specific surface area was calculated by the Brunaur–Emmett–Teller method. Solid-state ^{29}Si MAS NMR spectra (Bruker AV600, Germany) were acquired on a Bruker AV600 spectrometer.

2.5. Photocatalytic Degradation of RhB

The test of RhB degradation was carried out to evaluate the self-cleaning performance of TiO_2@SiO_2 and coated WC pastes. In photocatalytic tests of TiO_2@SiO_2 powders, P25 (0.01 g) and nanocomposites were dispersed in an RhB solution (20 mL, 10 mg/L), and the TiO_2 dosages of nanocomposites kept the same concentration. The suspension was further stirred for 30 min in the dark and was then irradiated by a UV lamp (20 W). Part of the solution (2 mL) was taken every 15 min until 105 min, and was centrifuged to remove nanocomposites. The concentration of the obtained solution was tested using a UV/Vis spectrometer at a wavelength of 463 nm to investigate the degradation efficiency. To measure the RhB degradation of coated WC pastes, the surface coated with nanocomposites was sprayed with 2 mL of RhB solution (80 mg/L). RhB contaminated specimens were irradiated by the UV lamp, and color variations (ΔE) before and after irradiation were recorded using a portable sphere spectrophotometer (RM200, X-Rite). The efficiencies of RhB removal was calculated by the comparison of the color variations before ($\Delta E(0)$) and after several hours ($\Delta E(t)$) of UV light irradiation. The detailed calculation method was mentioned in References [20,21].

A lab-simulated weathering system was used to mimic rain water in an outdoor environment. Circular tap water with a flow rate of 130 mm/h was produced by pumping it from a water tank in order to simulate the rain condition, and the process lasted 5 days.

3. Results and Discussion

TiO_2@SiO_2 nanocomposites with different coating thicknesses were prepared to investigate its effect on photocatalytic efficiency and the bonding force with the cement-based matrix. In order to obtain TiO_2@SiO_2 nanocomposites with different coating thicknesses, experimental parameters, such as the temperature and dosage ratio of TEOS and P25, were adjusted to prepare different nanocomposites. Samples 1, 3, 4, and 6 were selected to investigate the effect of experimental parameters on the coating thicknesses of TiO_2@SiO_2 nanocomposites. The TEM images of these nanocomposites are shown in Figure 1. Compared to the TEM images of four nanocomposites, the SiO_2 shell of Samples 1 and 4 is obviously present. The results indicate that the dosage ratio of TEOS and P25 decides the molar ratio of SiO_2 and TiO_2, and the higher value promotes the formation of the SiO_2 shell. The enlarged insets of Figure 1a,c and show that the two nanocomposites both have core-shell structures, and the main shell thicknesses of Samples 1 and 4 are about 3.92 and 6.13 nm, respectively. During the preparation process

of the coating, the rates of hydrolysis and condensation processes decreased at lower temperatures, and SiO_2 preferentially deposited on the surface of TiO_2 particles, benefiting the process of more coating.

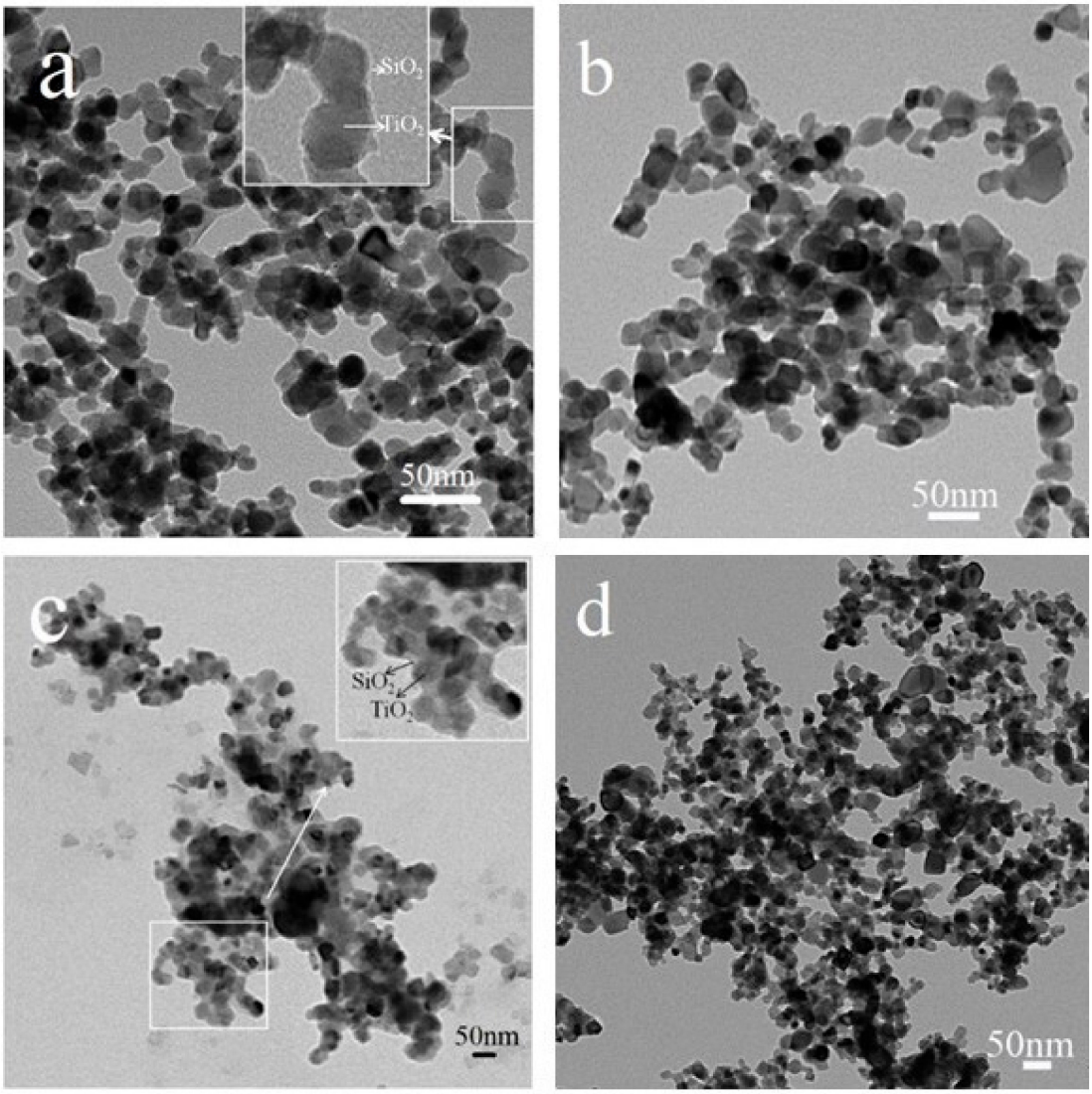

Figure 1. TEM images of Sample 1 (**a**), Sample 3 (**b**), Sample 4 (**c**), and Sample 6 (**d**).

The photocatalytic activities of TiO_2@SiO_2 nanocomposites with different shell thicknesses and P25 were evaluated by monitoring the degradation of RhB under UV-light irradiation, and the results are shown in Figure 2. After dark reaction for 30 min, the degradation rates of TiO_2@SiO_2 nanocomposites were higher than that of pure P25. Meanwhile, the values increase with the increase in the shell thickness, mainly owing to the absorption of the SiO_2 coating. Samples 2, 3, and 6 have higher degradation efficiencies than pure P25 when the irradiation time was 105 min, indicating that the SiO_2 coating accelerates RhB removal to a certain extent. This may be owing to the high surface area of SiO_2, which adsorbed more dyes to the benefit of more dye degradation [14]. Samples 1 and 4 have higher SiO_2 coating thicknesses, however, their photocatalytic efficiencies are the lowest. This is probably because much of the coating may hinder the transport of photons and decrease light absorption [18]. During the preparation process of TiO_2@SiO_2 nanocomposites, temperature may be an influencing factor for the thickness and density of the coating, which further affects the photocatlytic activity of nanocomposites. The nanocomposites prepared at 25 °C have higher degradation rates than nanocomposites synthetized at 0 °C, which may be due to the difference in the coating thickness and morphology.

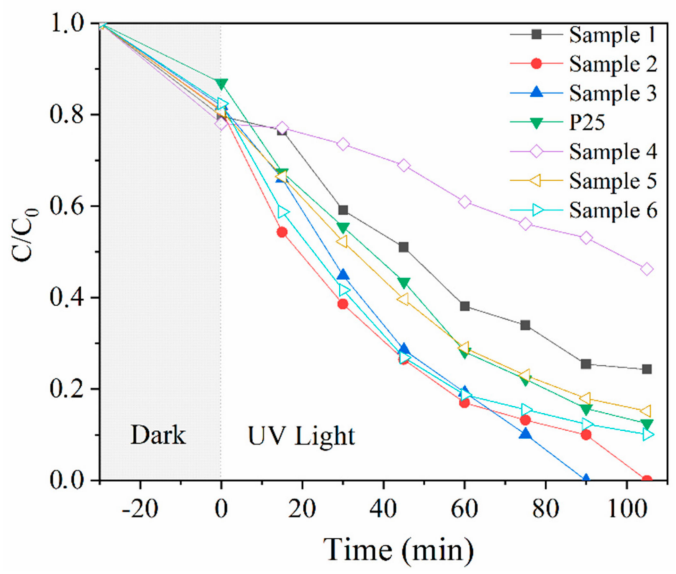

Figure 2. Photocatalytic degradation of RhB under UV light by P25 and TiO_2@SiO_2 nanocomposites.

Samples 1–3 and P25 were sprayed on the surface of WC pastes, and the specimens coated with Samples 1–6 and P25 were named WC 1–6 and WC P25, respectively. The surface microstructures are shown in Figure 3. The figures indicate that the surfaces of hardened cement pastes treated with Samples 1–3 are denser than those of untreated cement pastes and the paste treated with P25. The results may be due to the gelatinization of SiO_2 or the pozzolanic reaction of SiO_2 and cement matrix. The adding of SiO_2 shell improves the surface quality of cement-based materials, and it may protect against the release of TiO_2 in a harsh weathering environment. In order to investigate the photocatalytic properties of WC specimens, the RhB degradation rates of these specimens were first measured after the TiO_2@SiO_2 nanocomposites were sprayed on the surface of the WC pastes. After that, these specimens were put into a curing chamber for two weeks. TiO_2@SiO_2 nanocomposites may react with the WC matrix due to their pozzolanic activity, and the degradation rates were measured again to investigate the effect of reaction productions on the photocatalytic efficiency. If the pozzolanic reaction occurs, the production could decrease the release of TiO_2 after exposure to a harsh weathering process. Therefore, after the weather process, degradation rates of specimens were tested. The results are shown in Figure 4, and Table 3 shows the detailed data from the figure. RhB degradation rates of WC 1 and WC 4 are the highest, and the tendency is different from the degradation rates of TiO_2@SiO_2 nanocomposites. This probably because adsorption action is more effective on the RhB degradation after nanocomposites are applied on the surface of WC pastes. After curing, their degradation rates significantly increase. C-S-H gel with relatively larger BET surface areas may be formed due to the pozzolanic reaction, which may adsorb more RhB dye. The results indicate that the reaction production has no negative effect on photocatalytic efficiency. Instead, it increases BET surface areas to promote RhB degradation. The production may decrease the release of TiO_2 and improve the durability of photocatalytic activity. After the weather process, the RhB removals of all specimens were decreased, and the reduction of WC P25 was obvious. WC 1 and WC 4 show the minimum photocatalytic efficiencies, which was due to more SiO_2 coating of Samples 1 and 4. Meanwhile, WC 4 has the minimum value due to its larger thickness of the SiO_2 coating mentioned above. The results show that adding SiO_2 could improve the adhesion between the coating and substrates, and the durability of the photocatalytic property, in particular for a harsh weathering process. The RhB degradations of WC 2 and WC 3 are similar, mainly owing to their similar BET surface areas, as mentioned above.

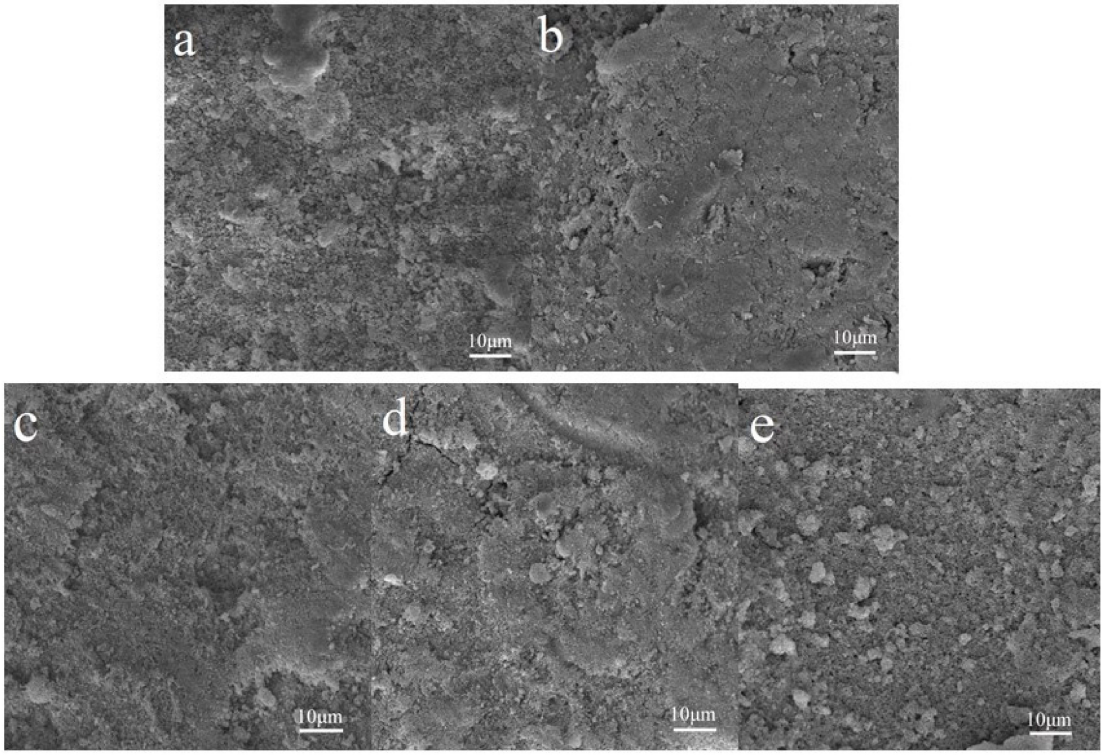

Figure 3. SEM images of harden cement pastes (**a**) and samples treated with Samples 1–3 (**b**–**d**) and P25 (**e**).

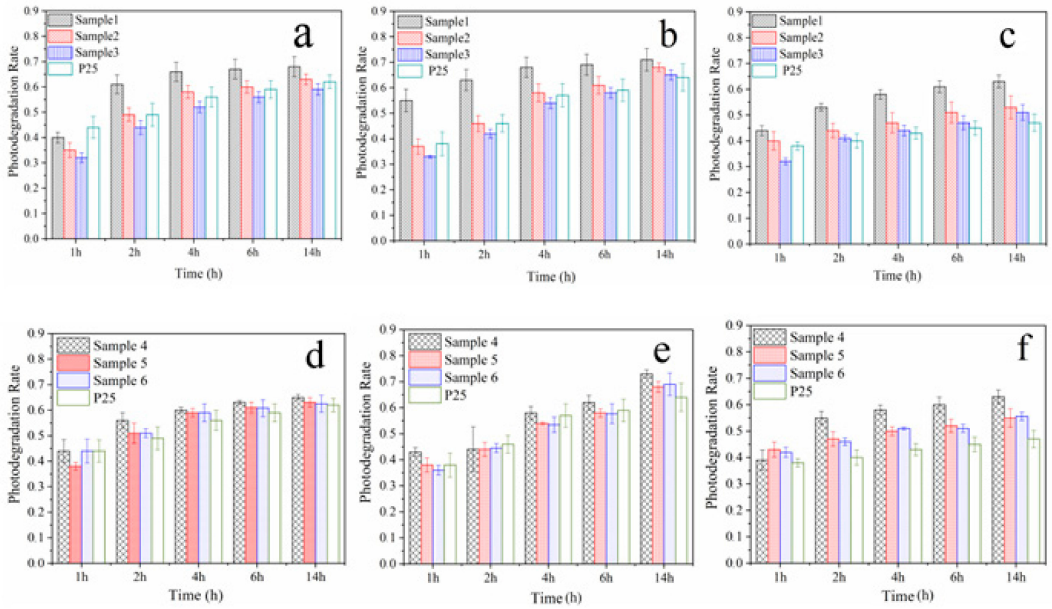

Figure 4. RhB degradation rates of WC 1-6 and WC P25 before (**a**,**d**) and after curing (**b**,**e**) and accelerated weather process (**c**,**f**).

Table 3. RhB degradation rates and reduction values of WC 1-6 and WC P25 after irradiation.

Sample	Sample 1	Sample 2	Sample 3	Sample 4	Sample 5	Sample 6	P25
Direct measurement	68.1%	63.1%	59.4%	65.0%	63.1%	62.5%	62.4%
After curing	71.5%	68.1%	65.0%	73.4%	68.0%	69.1%	64.0%
After weather process	62.9%	53.4%	51.0%	63.3%	55.0%	55.6%	47.4%
Reduction	7.6%	15.4%	14.1%	2.6%	12.8%	11.0%	24.0%

To more specifically study the pozzolanic reaction of TiO_2@SiO_2 nanocomposites with the cement matrix, experiments of nanocomposites with $Ca(OH)_2$ (a hydration product of cement) were carried out to investigate the formation of the reaction production. Sample 2 was selected and was mixed with $Ca(OH)_2$ saturated solution by stirring for seven days. TEM image of the reaction product of Sample 2 and $Ca(OH)_2$ is shown in Figure 5. A foil-like structure was formed after the reaction, which may be a C-S-H gel. The particles are deposited on the surface of a foil-like structure. The SiO_2 shell reacted with $Ca(OH)_2$, and the product core was first deposited on the particles. The product core further grew to a foil-like structure. This may explain why the adding of SiO_2 decreased the release of TiO_2 and improved the durability of the photocatalytic activity.

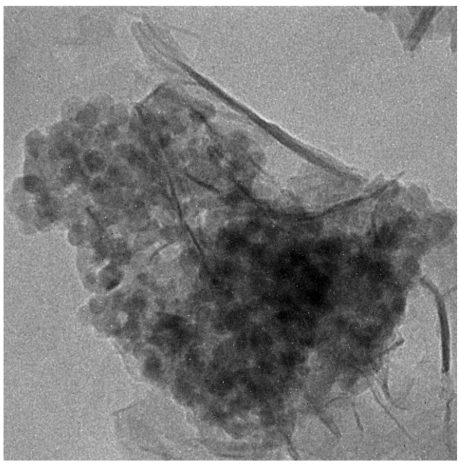

Figure 5. TEM image of reaction product of Sample 2 and $Ca(OH)_2$.

The objective of ^{29}Si NMR spectrum is to assess the composition of the foil-like structure and Q_n structure of the Si tetrahedron. Figure 6 shows the spectra of Sample 2 and its reaction production with $Ca(OH)_2$. The spectrum of Sample 2 shows two signals centered at 102.5 and 113.1 ppm, which were associated with the Q_3 and Q_4 units in the SiO_2 structure, according to previous reports [22,23]. After the reaction with Sample 2 and $Ca(OH)_2$, the two main peaks shifted to 81.7 and 88.0 ppm, which were assigned to Q^1 and Q^2 silicate connections. The results indicate a decrease in the polymerization degree of silicon and the formation of a C-S-H gel. After the reaction, the SiO_2 coating transformed to a C-S-H gel, which could decrease the release of TiO_2 after exposure to a harsh weathering process.

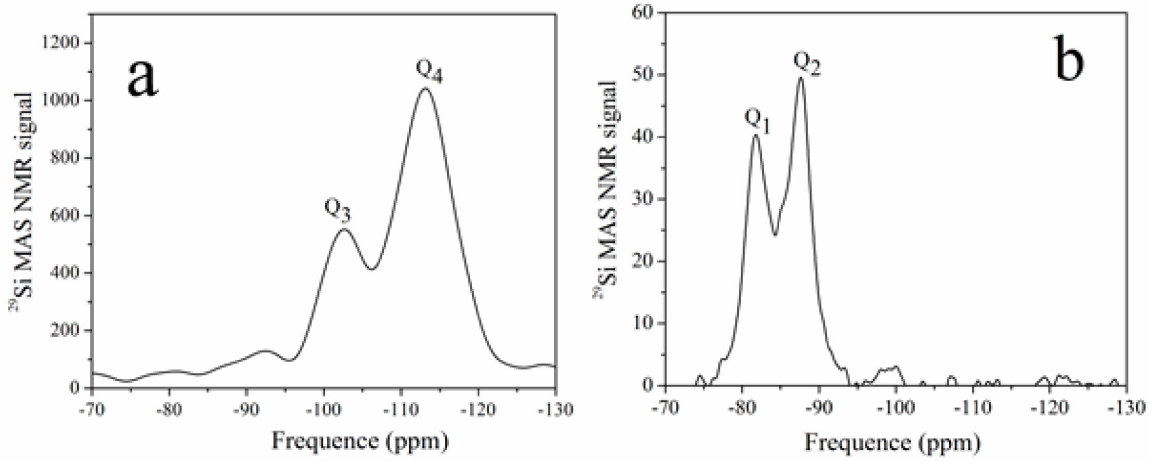

Figure 6. NMR spectra of Sample 2 (**a**) and its reaction production (**b**) with $Ca(OH)_2$.

4. Conclusions

TiO_2@SiO_2 nanocomposites were prepared using different experiment parameters, and their RhB degradations were measured. The results show that SiO_2 coating accelerates the RhB removal to a certain extent, owing to the high surface area of SiO_2, which adsorbed more dyes to the benefit of more dye degradation. More SiO_2 coating may hinder the transport of photons and decrease light absorption, which further decreases photocatalytic efficiencies. After these nanocomposites were applied on the surface of the WC pastes, their RhB degradation rates are higher than WC P25, which is probably because adsorption action is more effective on the RhB degradation. After curing, their degradation rates significantly increase. C-S-H with relatively large BET surface areas may be formed due to the pozzolanic reaction, which may adsorb more RhB dye. After the weather process, the RhB removals of all specimens decreased, and the reduction of WC P25 was obvious. Meanwhile, WC 4 has the minimum value. Adding SiO_2 could improve the adhesion between coating and substrates, and the durability of the photocatalytic property, in particular for a harsh weathering process. The experimental data of nanocomposites with $Ca(OH)_2$ further prove the formation of C-S-H gels and reveal the reaction of the mechanism of nanocomposites and the cement matrix.

Author Contributions: X.C. and D.W. conceived and designed the study; D.W. and Z.G. performed the experiments; D.W. wrote the paper; P.Y., S.H., and X.C. reviewed and edited the manuscript. Resourse: P.H. All authors have read and agreed to the published version of the manuscript.

Funding: This research was funded by the Program for Taishan Scholars Program, Case-by-Case Project for Top Outstanding Talents of Jinan, Distinguished Taishan Scholars in Climbing Plan, National Natural Science Foundation of China (Grant No. 51632003 and 51902129), the National Key Research and Development Program of China, (Grant No. 2016YFB0303505), and the 111 Project of International Corporation on Advanced Cement-based Materials (No. D17001).

Acknowledgments: This work was supported by the Program for Taishan Scholars Program, Case-by-Case Project for Top Outstanding Talents of Jinan, Distinguished Taishan Scholars in Climbing Plan, National Natural Science Foundation of China (Grant No. 51632003 and 51902129), the National Key Research and Development Program of China, (Grant No. 2016YFB0303505), and the 111 Project of International Corporation on Advanced Cement-based Materials (No. D17001).

Conflicts of Interest: The authors declare no conflict of interest.

References

1. Guo, M.Z.; Maury-Ramirez, A.; Poon, C.S. Self-cleaning ability of titanium dioxide clear paint coated architectural mortar and its potential in field application. *J. Clean Prod.* **2016**, *112*, 3583–3588. [CrossRef]
2. Chen, M.; Chu, J.W. NO_x photocatalytic degradation on active concrete road surface-from experiment to real-scale application. *J. Clean. Prod.* **2011**, *19*, 1266–1272. [CrossRef]
3. Guo, M.Z.; Maury-Ramirez, A.; Poon, C.S. Versatile photocatalytic functions of self-compacting architectural glass mortars and their inter-relationship. *Mater. Des.* **2015**, *88*, 1260–1268. [CrossRef]
4. Yousefi, A.; Allahverdi, A.; Hejazi, P. Effective dispersion of nano-TiO_2 powder for enhancement of photocatalytic properties in cement mixes. *Constr. Build Mater.* **2013**, *41*, 224–230. [CrossRef]
5. Cárdenas, C.; Tobón, J.I.; García, C.; Vila, J. Functionalized building materials: Photocatalytic abatement of NOx by cement pastes blened with TiO2 nanoparticles. *Constr. Build Mater.* **2012**, *36*, 820–825.
6. Chen, J.; Kou, S.C.; Poon, C.S. Photocatalytic cement-based materials: Comparison of nitrogen oxides and toluene removal potentials and evaluation of self-cleaning performance. *Build Environ.* **2011**, *46*, 1827–1833. [CrossRef]
7. Sugrañez, R.; Álvarez, J.I.; Cruz-Yusta, M.; Mármol, I.; Morales, J.; Vila, J.; Sánchez, L. Enhanced photocatalytic degradation of NOx gases by regulating the microstructure of mortar cement modified with titanium dioxide. *Build Environ.* **2013**, *69*, 55–63. [CrossRef]
8. Sun, J.F.; Xu, K.; Shi, C.Q.; Ma, J.; Li, W.F.; Shen, X.D. Influence of core/shell TiO_2@SiO_2 nanoparticles on cement hydration. *Constr. Build Mater.* **2017**, *156*, 114–122. [CrossRef]
9. Tiainen, H.; Wiedmer, D.; Haugen, H.J. Processing of highly porous TiO_2 bone scaffolds with improved compressive strength. *J. Eur. Ceram Soc.* **2013**, *33*, 15–24. [CrossRef]

10. Ruot, B.; Plassais, A.; Olive, F.; Guillot, L.; Bonafous, L. TiO_2-containing cement pastes and mortars: Measurements of the photocatalytic efficiency using a rhodamine B-based colourimetric test. *Sol. Energy* **2009**, *83*, 1794–1801. [CrossRef]
11. Folli, A.; Pade, C.; Hansen, T.B.; Marco, T.D.; Macphee, D.E. TiO_2 photocatalysis in cementitious systems: Insights into self-cleaning and depollution chemistry. *Cem. Concr. Res.* **2012**, *42*, 539–548. [CrossRef]
12. Rachel, A.; Subrahmanyam, M.; Boule, P. Comparison of photocatalytic efficiencies of TiO_2 in suspended and immobilised form for the photocatalytic degradation of nitrobenzenesulfonic acids. *Appl. Cat. B Environ.* **2002**, *37*, 301–308. [CrossRef]
13. Martinez, T.; Bertron, A.; Escadeillas, G.; Ringot, E.; Simon, V. BTEX abatement by photocatalytic TiO_2-bearing coatings applied to cement mortars. *Build Environ.* **2014**, *71*, 186–192. [CrossRef]
14. Kamaruddin, S.; Stephan, D. Quartz-titania composites for the photocatalytical modification of construction materials. *Cem. Concr. Comp.* **2013**, *36*, 109–115. [CrossRef]
15. Kamaruddin, S.; Stephan, D. Sol-gel Mediated Coating and Characterization of Photocatalytic Sand and Fumed Silica for Environmental Remediation. *Water Air Soil Pollut.* **2014**, *225*, 1948. [CrossRef]
16. Hendrix, Y.; Lazaro, A.; Yu, Q.; Brouwers, J. Titania-Silica Composites: A Review on the Photocatalytic Activity and Synthesis Methods. *World J. Nano Sci. Eng.* **2015**, *5*, 161–177. [CrossRef]
17. Kamaruddin, S.; Stephan, D. The preparation of silica-titania core-shell particles and their impact as an alternative material to pure nano-titania photocatalysts. *Catal. Today* **2011**, *161*, 53–55. [CrossRef]
18. Mendoza, C.; Vallea, A.; Castellote, M.; Bahamondea, A.; Faraldosa, M. TiO_2 and TiO_2-SiO_2 coated cement: Comparison of mechanic and photocatalytic properties. *Appl. Catal. B Environ.* **2015**, *178*, 155–164. [CrossRef]
19. Sikora, P.; Cendrowski, K.; Markowska-Szczupak, A.; Horszczaruk, E.; Mijowska, E. The effects of silica/titania nanocomposite on the mechanical and bactericidal properties of cement mortars. *Constr. Build Mater.* **2017**, *150*, 738–746. [CrossRef]
20. Wang, D.; Hou, P.K.; Yang, P.; Cheng, X. BiOBr@SiO_2 flower-like nanospheres chemically-bonded on cement-based materials for photocatalysis. *Appl. Surf. Sci.* **2018**, *430*, 539–548. [CrossRef]
21. Wang, D.; Hou, P.K.; Zhang, L.N.; Yang, P.; Cheng, X. Photocatalytic and hydrophobic activity of cement-based materials from benzyl-terminated-TiO_2 spheres with core-shell structures. *Constr. Build Mater.* **2017**, *148*, 176–183. [CrossRef]
22. Vinogradova, E.; Estrada, M.; Moreno, A. Colloidal aggregation phenomena: Spatial structuring of TEOS-derived silica aerogels. *J. Colloid Interface Sci.* **2006**, *298*, 209–212. [CrossRef] [PubMed]
23. Humbert, B. Estimation of hydroxyl density at the surface of pyrogenic silicas by complementary NMR and Raman experiments. *J. Non-Cryst. Solids* **1995**, *191*, 29–37. [CrossRef]